Research Article | Vol. 27, No. 15 / 22 July 2019 / Optics Express 21358

Optics EXPRESS

Open-path multi-species remote sensing with a broadband optical parametric oscillator

OGUZHAN KARA,[1] FRAZER SWEENEY,[1] MARIUS RUTKAUSKAS,[1] C. FARRELL,[2] C. G. LEBURN,[2] AND DERRYCK T. REID[1,*]

[1]*Scottish Universities Physics Alliance (SUPA), Institute of Photonics and Quantum Sciences, School of Engineering and Physical Sciences, Heriot–Watt University, Edinburgh EH14 4AS, UK*

[2]*Chromacity Ltd. Livingstone House, 43 Discovery Terrace, Research Avenue North, Riccarton, Edinburgh, EH14 4AP, UK*

[*]*D.T.Reid@hw.ac.uk*

Abstract: Open-path remote sensing is critical for monitoring fugitive emissions from industrial sites, where a variety of volatile organic compounds may be released. At ranges of only a few tens of metres, spatially coherent broadband mid-infrared sources can access sufficiently large absorption cross-sections to quantify hydrocarbon gas fluctuations above ambient background levels at high signal:noise ratios. Here we report path-integrated simultaneous concentration measurements of water, methane and ethane implemented in the 3.1–3.5-μm range using 0.05-cm^{-1}-resolution Fourier-transform spectroscopy with an ultrafast optical parametric oscillator and a simple, non-compliant target. Real-time concentration changes were observed at a range of 70 m by simulating a fugitive emission with a weak localized release of 2% methane in air. Spectral averaging yielded a methane detection sensitivity of 595 ppb·m, implying a system capability to resolve few-ppb concentrations of many volatile organic compounds at observation ranges of 50–100 m.

1. Introduction

Fugitive hydrocarbon emissions cost the energy sector $5B per year, account for 12% of greenhouse gas emissions and jeopardize safety and public health. The most advanced technique for remote emission measurements is differential absorption lidar (DIAL), in which intense infrared (IR) pulses originating from a narrow-line source such as an optical parametric oscillator (OPO) [1,2] are directed into the atmosphere and returned to a ground-based detector by weak scattering from airborne particles. Notably, DIAL provides a range-gating capability [3], and the technique has been developed in several forms [4–6], including recently extending DIAL to multi-species measurements [7,8]. DIAL is characterized by the need for multi-mJ lasers, which can be large and inconvenient to operate and maintain. By contrast, Fourier transform infrared (FTIR) spectroscopy is naturally broadband and offers far wider coverage to DIAL, and in an open-path embodiment can detect hundreds of atmospheric gases with a small system footprint but normally without a range-gating capability. Active open-path mid-IR Fourier-transform spectroscopy using thermal sources [9–11] is already used for quantitative hydrocarbon emissions monitoring in and around petrochemical sites, at landfill sites and in agricultural contexts, typically proceeding at resolutions around 0.5 cm^{-1} [12], sufficient for species identification but presenting difficulties when absorption lines of multiple species are spectrally overlapped. Laser-based active FTIR spectroscopy offers higher resolution, providing the capability to distinguish similar gases such as methane and ethane, for example making it possible to separate petrochemical methane contributions—which are accompanied by a weak ethane signature—from biogenic sources (cattle, landfill, compost) which produce only methane.

#366400 https://doi.org/10.1364/OE.27.021358
Journal © 2019 Received 30 Apr 2019; revised 18 Jun 2019; accepted 19 Jun 2019; published 16 Jul 2019

Optics EXPRESS

Quantitative high resolution open-path gas sensing was first achieved in the near-infrared using an Er:fiber dual-comb system which provided 100-MHz resolution spectroscopy of CO_2, CH_4, H_2O, HDO and $^{13}CO_2$ across a 2 km path [13]. This was followed by a demonstration in the mid-infrared at 3.25 µm using a single Yb:laser-pumped OPO to measure atmospheric water and methane over a 26-m path at 700-MHz resolution with a virtually imaged phase array spectrometer [14]. In this article we present an eye-safe active FTIR spectroscopy system based on a broadband ultrafast OPO operating in the 3.1–3.5-µm wavelength range and capable of acquiring sub-0.1-cm^{-1} resolution gas absorption spectra from a simple target at ranges exceeding 70 meters. In contrast to previous work which employed optical quality targets (plane mirrors or retroreflectors) to return the beam, the combination of sufficient collection aperture, laser power and detector sensitivity allows us to obtain high quality spectroscopy from simple scattering targets such as aluminum foil, paper or concrete. Simultaneous quantitative measurement of atmospheric background levels of water and methane is demonstrated, even in the presence of strong absorption from a control cell of 1.5 ± 0.15% ethane gas, and the system is shown to be capable of real-time measurement of a localized 2% methane emission at a range of 65 m.

2. Experiment

2.1. OPO spectrometer

The light source was an ultrafast OPO (Spark-OPO, Chromacity Ltd. [15]) based on a fan-out MgO:PPLN crystal, which provided 100-MHz pulses with tunability from 2800–3900 nm and broad spectra as shown in Fig. 1. To access the strongest absorptions in methane and ethane we selected a grating position that provided instantaneous coverage from 3.1–3.5 µm, with an average power >300 mW and a 1-cm-diameter beam with a measured M^2 value of 1.05.

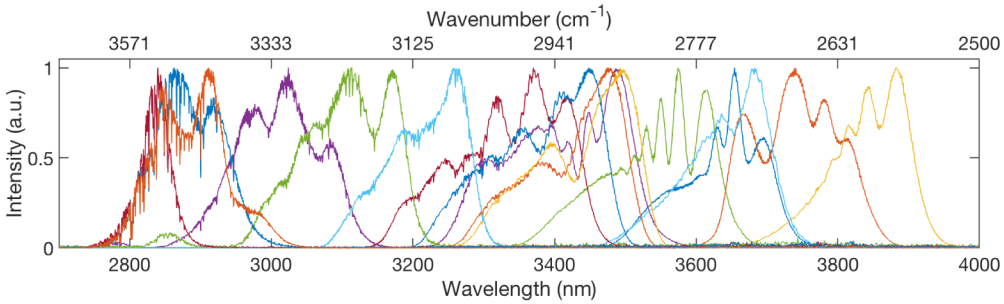

Fig. 1. Idler spectra produced by fan-out-grating tuning of the MgO:PPLN crystal. The spectral shapes are determined by the phasematching characteristics of the MgO:PPLN crystal and by the OPO pump-laser spectrum. Water absorption lines are visible at shorter wavelengths.

The spectrometer (Fig. 2) was based on a design described in [16], in which the OPO light was first coupled into a scanning Michelson interferometer before being launched into free-space and subsequently collected by a 6-inch f/4 Newtonian telescope after scattering from a remote target. The returned light was detected using an InSb liquid-nitrogen-cooled photodiode situated at the telescope focus. Light from the OPO was launched along an optical axis co-aligned with the telescope's field of view using a small 45° steering mirror situated directly before the secondary mirror of the telescope. The scanning interferometer operated at 1 Hz and achieved a typical resolution of 0.05 cm^{-1}, which is sufficient to resolve the narrow and complex absorption-line structure of light molecules like water, methane and ethane. The entire system was constructed on a 60 × 90 cm breadboard and mounted on a trolley.

Optics EXPRESS

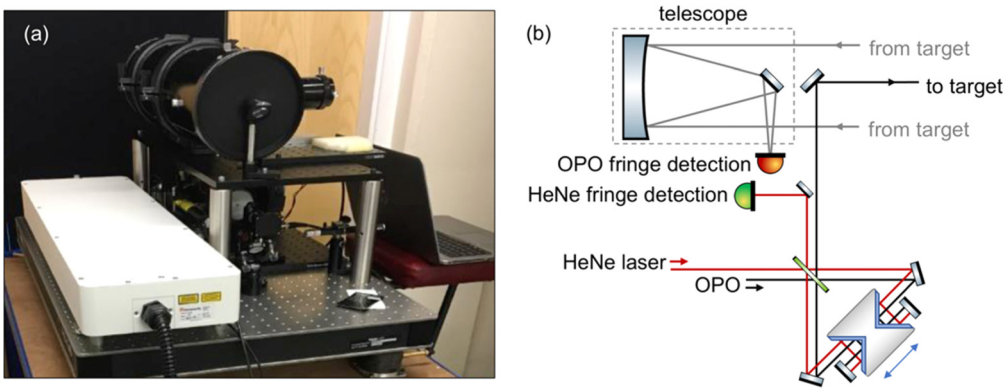

Fig. 2. (a) OPO, telescope and scanning Michelson interferometer on a 60×90 cm breadboard. (b) Layout of the Fourier-transform spectrometer.

2.2. Simultaneous methane, ethane and water measurement at 30-m range

To establish the ability to measure multiple spectrally-overlapping species simultaneously, we performed indoor measurements from a rough Al-foil target at a range of up to 30 meters, in which the light launched from the OPO entered a 20-cm-long gas cell containing a $1.5 \pm 0.15\%$ ethane-in-air mixture and situated directly in front of the secondary mirror of the collection telescope. Figure 3(a) (blue) displays an example of a single measured spectrum (no averaging) exhibiting densely packed absorption lines from water, methane and ethane, as well as continuum absorption from ethane, which suppresses the overall spectral intensity.

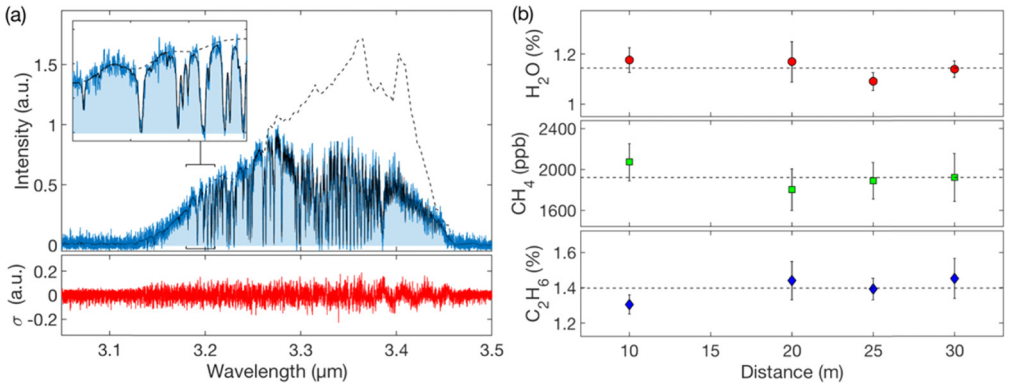

Fig. 3. (a) Example spectrum from a set of 45 collected at 30-m range from a rough aluminum-foil target. The upper plot shows the envelope of the illumination spectrum extracted from a fitting procedure which simultaneously minimized the rms error between the experimental spectrum (blue) and a synthetic spectrum (black) calculated from the envelope and a fitted mixture of PNNL absorbance data for water, methane and ethane. In this example the best-fit concentrations determined were 1.15% (water), 1860 ppb (methane) and 1.37% (ethane). The lower plot shows the rms fitting residual. (b) Measured concentrations at 10, 20, 25 and 30 m, with data points showing the average values from approximately 45 spectra each, and the error bars showing the ± 1 standard deviation range. The methane background value is consistent with reported ambient levels measured at 1885 ± 15 ppb [17]. Respective water and ethane values were consistent with the ambient relative humidity measured in the building and the filling concentration of the ethane cell. The dashed lines show the average of all the measured values.

Optics EXPRESS

Quantitative open-path spectroscopy requires either a reliable reference spectrum or a method of inferring the original illumination spectrum, and this problem has been treated in different ways in previously reported studies [13,14]. The approach used is described in the Appendix and results in the retrieval of an illumination spectrum (Fig. 3(a), dashed line) which represents the OPO output spectrum prior to undergoing atmospheric absorption. The black line in Fig. 3(a) is the best-fit absorption spectrum using 0.1-cm^{-1}-resolution PNNL database data [18] as the fitting reference. The residual (Fig. 3(a), red) shows some deviations of order similar to the rms noise near the spectral lines due to mismatch between the measured line shapes and the PNNL data. The inset in Fig. 3(a) shows the typical correspondence between the measured spectrum and the best-fit data. Figure 3(b) shows the extracted concentration data for water, methane and ethane, showing that it is possible to obtain environmental concentration values consistent with independent humidity measurements (water), established ambient levels (methane) or known control concentrations (ethane).

2.3. *Real-time methane emission measurement at 70-m range*

Using a 78-m indoor corridor as a test site we simulated a point emission by releasing a 2% methane:air mix for 100 seconds at a rate of 103 µg s^{-1} at a distance of 65 m from the OPO. The signal was recorded from a simple target of rough aluminum foil situated 70 meters from the OPO, with the beam passing near the emission point. No ethane cell was present. Spectra recorded every seven seconds were fitted in the same way as described previously to provide concentrations of water, methane and ethane. Although ethane concentration remained as an available fitting parameter, as expected the resulting fitted concentration was negligible since ethane is not naturally present in the atmosphere. Figure 4(a) shows an example of a spectrum recorded without averaging at 70-m range and at a moment close to the peak methane emission. The Q-branch of methane can be clearly seen near 3.31 µm. The inset of Fig. 4(a) shows the correspondence to the best-fit PNNL database in the 3.18–3.21-µm region. In contrast to ethane, methane and water show very little continuum absorption under these experimental conditions (20°C, 101800Pa), so the inferred illumination spectrum closely follows the envelope of the measured spectrum. Figure 4(b) presents the measured water and methane concentrations over 400 seconds, showing the methane concentration rising from background levels (~1900 ppb) to a peak of around 13000 ppb before returning to near the original value as the gas disperses. Prior to the methane release, the rms variation of the measured concentration of background methane

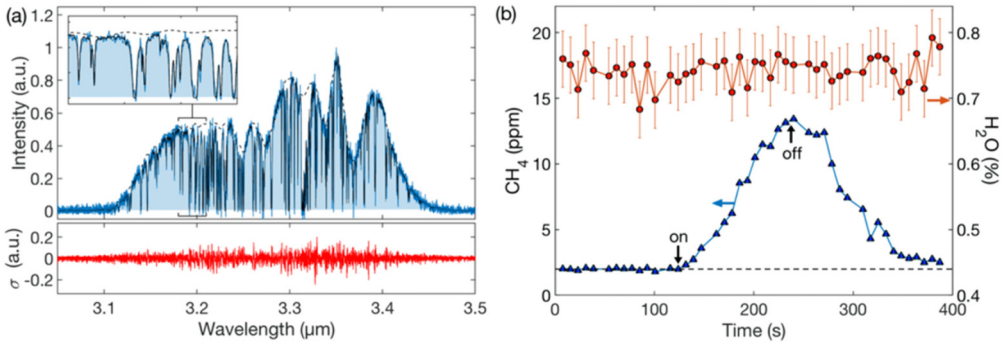

Fig. 4. (a) Example spectrum from a set of 51 collected at 70-m range from a rough aluminum-foil target. In this example the best-fit concentrations were 0.77% water, 12650 ppb methane and 0% ethane. (b) Concentrations of methane (blue) and water (red) measured before, during and after the methane release, showing a recovery to near-background levels after 150 seconds.

Optics EXPRESS

at this range was <100 ppb. Water showed more variability, which is expected to be associated with convection effects and environmental variations.

2.4. Detection sensitivity, repeatability and accuracy

Sensitivity to path integrated concentrations of a few ppb can be achieved by averaging multiple spectra. Using a 35-m-range aluminum-foil target, and with the OPO tuned away from the strongest methane and water absorption lines, we averaged 1250 spectra over one hour to obtain the spectrum shown in Fig. 5. As before, the dashed line is the fitted illumination spectrum, the blue line and fill depicts the (averaged) experimental data and the black line is the combined envelope and absorption-line fit, in this case using HITRAN data [19] for methane, water-vapor and carbon dioxide. The use of HITRAN avoided an artefact in the PNNL data which introduced a weak continuum absorption in methane, of minimal impact when fitting individual spectra but observable when fitting a low-noise averaged spectrum. The quality of the fit can be seen from the inset, which compares the fitted and average spectra, with a 0.1-cm^{-1} instrument response imposed on the HITRAN data. The best-fit concentrations were 0.977% water, 1830 ppb methane and no carbon dioxide (as expected in this wavelength band). Small differences between the experimental and HITRAN line shapes are observed in the residuals. The rms error in absorption-free regions (e.g. line-free wavelengths from 3.15–3.20 μm) is 0.19%, and using a representative absorption feature at 3.1847nm, for which $\alpha = 0.0391$ at 1.8 ppm, this figure implies—via consideration of the noise-limited minimum observable transmission change—a detection sensitivity for methane of 97 ppb. Tuning the OPO to 3.3 μm encounters the strongest methane absorption (the Q-branch, for which $\alpha = 0.217$ at 1.8 ppm), and at this wavelength the equivalent detection sensitivity would be 17 ppb (or 595 ppb·m). A comparison can be made with commercial open-path Fourier-transform spectrometers, for which a survey of 64 common gases [20] reported a sensitivity of 1597 ppb·m for methane measurements near 3017 cm^{-1} (Q-branch absorption). A leading commercial system reports 2 ppb detection sensitivity for methane at 200

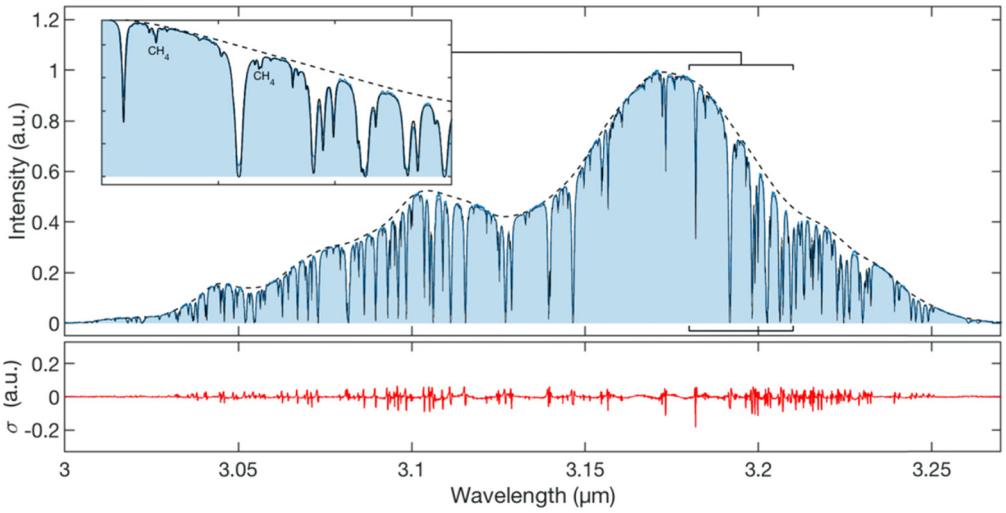

Fig. 5. Average of 1250 spectra acquired over a 35-m indoor range (blue and shaded), and a comparison with the best-fit HITRAN data (black) for 0.977% water vapor and 1830 ppb methane. The co-fitted illumination envelope is indicated by the dashed line. Most of the lines are from water, but the small features labelled in the inset (3.18–3.21 μm) are two of the most prominent methane absorptions. The residual (red) reveals remaining line-shape fitting errors.

Optics EXPRESS

m range with 1 hour of averaging [21]. Scaling our 1-hour-averaging results from 35 m to 200 m implies an equivalent performance of 1.5 ppb, but critically this is achieved without the need for a precision retroreflector-array target.

While averaging is advantageous from a noise point of view, the stability of the atmosphere ultimately limits the accuracy and repeatability of the measurements which can be obtained. All the measurements reported here were performed indoors, where convection and temperature changes were the principal causes of fluctuations in the concentrations and/or absorbances of ambient water vapor and methane. Using the same dataset as in Fig. 5, we present in Figs. 6(a) and 6(b) the results of individual fits to each spectrum, showing mean concentrations and standard deviations for methane and water vapor of 1861 ± 349 ppb and 0.963 ± 0.0725% respectively. Around 200 spectra for which the fitting error was exceptionally high were removed prior to the analysis. The mean concentration values agree closely with the best fit concentrations of the average spectrum (Fig. 5). The Allan deviation [Fig. 6(c)] provides an insight into the stability and repeatability of the measurements, showing that averaging around 100 results (~ 5 minutes of acquisition time) provides the greatest repeatability, but with longer acquisitions showing slightly higher fluctuations in the mean, particularly for water vapor, whose concentration changes sensitively with temperature. A trade-off between repeatability and sensitivity is therefore encountered at acquisition times above 5–10 minutes.

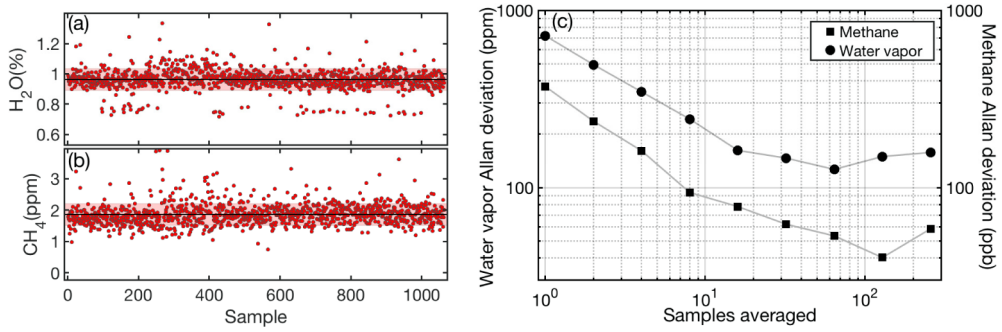

Fig. 6. Results of fitting to 1063 individual spectra acquired over a 35-m indoor range, showing concentrations for (a) water vapor (9634 ± 725 ppm) and (b) methane (1861 ± 349 ppb), with ± one standard deviation shown by the shaded regions. (c) Allan deviation analysis.

3. Summary and conclusions

The demonstrated system offers several advantages to previously reported open-path sensing of atmospheric species. The measurements conducted here were carried out with very simple, alignment-free targets, typically a coarsely positioned sheet of aluminum foil at a range of up to 70 m, but also with returns from > 30 m available from paper, laminate or similar targets. Indeed, the range limit in our experiments was imposed by the dimensions of the building available and, based on the signal:noise performance which we obtained, we expect that a range of between 150–200 m would be possible with no modification of the equipment. Our results can be compared with the performance of alternative laser technologies. Sensing of methane, water and carbon dioxide at background concentration levels and using simple reflective-tape targets to achieve km-level ranges was reported using a MgO:PPLN OPA system operating at several discrete wavelengths [22], while a narrow-line OPO in a master-oscillator power amplifier configuration tuning from 3.3–3.7 μm achieved methane and water measurements at 30-m range from a topographic target [23]. Quantum cascade lasers (QCLs) were used for stand-off detection of water vapor, methane, nitrous oxide, and hydrogen peroxide near 8 μm and at 30.2-m range

Optics EXPRESS

using a painted wooden target [24], and methanol / ethanol plumes were detected at 10-m range using a brushed Al target and a QCL operating near 10 µm [25]. In-the-field FTIR spectroscopy using thermal sources always requires high-quality retroreflecting targets, so the ability to use a simple topographic target increases the practicality of the system, since it both relaxes the beam pointing accuracy needed (there is no need to maintain the beam on a small retroreflector) and in some cases eliminates altogether the need for a remote target. A highlight of the system's performance is its ability to extract concentration data from a single spectrum with no need for averaging, which provides a real-time and quantitative monitoring capability and, as described in Section 2.3, makes the system suitable for detecting weak, localized emissions. While not achieving the resolution which is possible using dual-comb spectroscopy [13], the resolution of ~0.05 cm^{-1} has been shown to be sufficient for extracting concentration measurements from complex, spectrally overlapping multiple species. Combined with the real-time monitoring capabilities of the system, this feature could permit correlations between different hydrocarbon gas concentrations to be observed, providing insights into their origin. Finally, we note that open path sensing requires an eye-safe capability. With the current beam parameter, ranges of >10 m from the OPO aperture are eye-safe for prolonged exposure, corresponding to an irradiance of <0.1 W cm^{-1} in this wavelength band [26].

Appendix: Illumination envelope extraction

The Beer-Lambert law describes the absorbance in terms of the light intensity before (I_o) and after (I) an absorbing medium, according to $I = I_o \exp(-\alpha)$, where I, I_o and α are functions of wavelength. Quantitative spectroscopy relies on inverting the Beer-Lambert law to obtain the absorbance, $\alpha = -\log(I/I_o)$, which requires accurate knowledge of the illumination intensity before the sample. In a laboratory measurement, a spectrum can be recorded without the sample and another with the sample present, but in a remote sensing context it is impossible to run a control experiment where the atmosphere is absent, so this option is unavailable. An alternative laboratory approach employs a reference detector to record the instantaneous intensity of the illumination source (I_o) in tandem with the intensity after the sample (I), so providing the desired I/I_o ratio. In a free-space atmospheric measurement, this approach also fails because a local reference detector cannot account for systematic effects like unknown contributions to the spectral envelope of the light from the scattering target or the propagation path.

To learn the effective illumination spectrum the solution is to allow I_o to be an additional free parameter when fitting the molecular absorbances to the measured spectrum, however fitting a structured spectral envelope from a broadband OPO is challenging, since it must be described by many more free points than the gas absorbances, which (neglecting temperature and pressure corrections) need just one number per gas species fitted. Performing a global multi-point optimization from a naïve initial guess is slow and failure-prone because of many local minima in the optimization landscape. Instead, we first obtain a rapid, accurate estimate of I_o and the absorbance values from a piecewise fitting of small fragments of the measured spectrum then use these as a robust starting point to refine the values in a full-spectrum fit. This approach combines the baseline removal reported for free-space spectroscopy using dual combs at 1.55 µm [13] and the global optimization used in dual-comb spectroscopy [27] with OPGaP OPOs [28]. For species like water and methane that exhibit no band-continuum absorption we note that another strategy is to reconstruct an envelope from the points between the absorption lines [14], but this approach cannot deal with spectra from heavier alkanes like ethane and propane.

Illustrated in Fig. 7, the algorithm begins by estimating the gas concentrations from a rapid initial fitting, carried out by dividing the spectrum into N fragments of approximately 1-cm^{-1} extent and performing a simple $(n+1)$-parameter fit of the absorbance coefficients $c_1 \ldots c_n$ of n gases and the illumination intensity, c_0. Thus, for the water, methane and ethane fitting used here $n = 3$. An initial estimate of the complete illumination spectrum (I_o) is provided by concatenating

Optics EXPRESS

the set of c_0 values, and the fitting concentrations are obtained from a weighted average of the set of $\{c_1 \ldots c_n\}$ parameters, favoring regions of the spectrum with greater intensities by using a function $F(c_0)$ such as ${c_0}^3$. These estimates provide a robust starting point for a global optimization that refines the gas concentration values using the entire broadband spectrum, in which the illumination spectrum is modelled as a many-point spline function and is co-optimized with the concentrations of all the participating gas species. The initial estimate is very rapid, taking a few seconds in MATLAB, with the global optimization taking around one minute and up to a few hundred iterations.

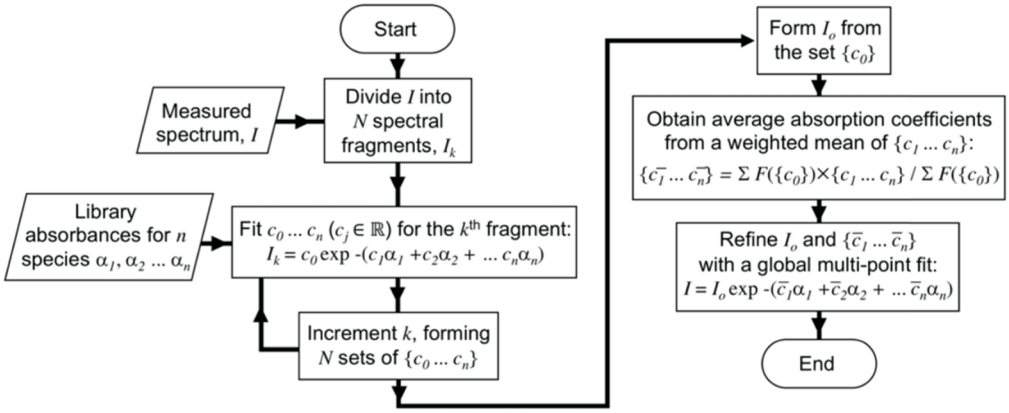

Fig. 7. Illumination envelope extraction algorithm. See text for details.

Funding

Science and Technology Facilities Council (STFC) (ST/P00699X/1).

References

1. T. Henningsen, M. Garbuny, and R. L. Byer, "Remote detection of CO by parametric tunable laser," Appl. Phys. Lett. **24**(5), 242–244 (1974).
2. M. Endemann and R. L. Byer, "Simultaneous remote measurements of atmospheric temperature and humidity using a continuously tunable IR lidar," Appl. Opt. **20**(18), 3211–3217 (1981).
3. D. J. Brassington, "Differential absorption lidar measurements of atmospheric water vapor using an optical parametric oscillator source," Appl. Opt. **21**(24), 4411–4416 (1982).
4. M. J. Milton, T. Gardiner, F. Molero, and J. Galech, "Injection-seeded optical parametric oscillator for range-resolved DIAL measurements of atmospheric methane," Opt. Commun. **142**(1-3), 153–160 (1997).
5. G. Poberaj, A. Fix, A. Assion, M. Wirth, C. Kiemle, and G. Ehret, "Airborne all-solid-state DIAL for water vapour measurements in the tropopause region: system description and assessment of accuracy," Appl. Phys. B: Lasers Opt. **75**(2-3), 165–172 (2002).
6. P. Weibring, H. Edner, and S. Svanberg, "Versatile mobile lidar system for environmental monitoring," Appl. Opt. **42**(18), 3583–3594 (2003).
7. G. A. Wagner and D. F. Plusquellic, "Multi-frequency differential absorption LIDAR system for remote sensing of CO_2 and H_2O near 16 µm," Opt. Express **26**(15), 19420–19434 (2018).
8. E. Cadiou, D. Mammez, J.-B. Dherbecourt, G. Gorju, J. Pelon, J.-M. Melkonian, A. Godard, and M. Raybaut, "Atmospheric boundary layer CO_2 remote sensing with a direct detection LIDAR instrument based on a widely tunable optical parametric source," Opt. Lett. **42**(20), 4044–4047 (2017).
9. T. L. Marshall, C. T. Chaffin, R. M. Hammaker, and W. G. Fateley, "An introduction to open-path FT-IR atmospheric monitoring," Environ. Sci. Technol. **28**(5), 224A–232A (1994).
10. C. Schütze, S. Lau, N. Reiche, U. Sauer, H. Borsdorf, and P. Dietrich, "Ground-based remote sensing with open-path fourier- transform infrared (OP-FTIR) spectroscopy for large-scale monitoring of greenhouse gases," Energy Procedia **37**, 4276–4282 (2013).
11. T. E. L. Smith, M. J. Wooster, M. Tattaris, and D. W. T. Griffith, "Absolute accuracy and sensitivity analysis of OP-FTIR retrievals of CO_2, CH_4 and CO over concentrations representative of 'clean air' and 'polluted plumes'," Atmos. Meas. Tech. **4**(1), 97–116 (2011).

Optics EXPRESS

12. K. C. Cossel, E. M. Waxman, I. A. Finneran, G. A. Blake, J. Ye, and N. R. Newbury, "Gas-phase broadband spectroscopy using active sources: progress, status, and applications [Invited]," J. Opt. Soc. Am. B **34**(1), 104–129 (2017).
13. G. B. Rieker, F. R. Giorgetta, W. C. Swann, J. Kofler, A. M. Zolot, L. C. Sinclair, E. Baumann, C. Cromer, G. Petron, C. Sweeney, P. P. Tans, I. Coddington, and N. R. Newbury, "Frequency-comb-based remote sensing of greenhouse gases over kilometer air paths," Optica **1**(5), 290–298 (2014).
14. L. Nugent-Glandorf, F. R. Giorgetta, and S. A. Diddams, "Open-air, broad-bandwidth trace gas sensing with a mid-infrared optical frequency comb," Appl. Phys. B: Lasers Opt. **119**(2), 327–338 (2015).
15. Full laser specifications are available from the manufacturer's website: http://www.chromacitylasers.com/
16. L. Maidment, Z. Zhang, C. R. Howle, and D. T. Reid, "Stand-off identification of aerosols using mid-infrared backscattering Fourier-transform spectroscopy," Opt. Lett. **41**(10), 2266–2269 (2016).
17. E. J. Dlugokencky, A.M. Crotwell, P.M. Lang, J.W. Mund, and M.E. Rhodes, "Atmospheric methane dry air mole fractions from quasi-continuous measurements at Barrow, Alaska and Mauna Loa, Hawaii, 1986-2017," Version: 2018-03-19, Path: ftp://aftp.cmdl.noaa.gov/data/trace_gases/ch4/in-situ/surface/ (2018).
18. S. W. Sharpe, T. J. Johnson, R. L. Sams, P. M. Chu, G. C. Rhoderick, and P. A. Johnson, "Gas-phase databases for quantitative infrared spectroscopy," Appl. Spectrosc. **58**(12), 1452–1461 (2004).
19. L. S. Rothman, I. E. Gordon, Y. Babikov, A. Barbe, D. Chris Benner, P. F. Bernath, M. Birk, L. Bizzocchi, V. Boudon, L. R. Brown, A. Campargue, K. Chance, E. A. Cohen, L. H. Coudert, V. M. Devi, B. J. Drouin, A. Fayt, J.-M. Flaud, R. R. Gamache, J. J. Harrison, J.-M. Hartmann, C. Hill, J. T. Hodges, D. Jacquemart, A. Jolly, J. Lamouroux, R. J. Le Roy, G. Li, D. A. Long, O. M. Lyulin, C. J. Mackie, S. T. Massie, S. Mikhailenko, H. S. P. Müller, O. V. Naumenko, A. V. Nikitin, J. Orphal, V. Perevalov, A. Perrin, E. R. Polovtseva, C. Richard, M. A. H. Smith, E. Starikova, K. Sung, S. Tashkun, J. Tennyson, G. C. Toon, V. G. Tyuterev, and G. Wagner, "The HITRAN2012 molecular spectroscopic database," J. Quant. Spectrosc. Radiat. Transfer **130**, 4–50 (2013).
20. G. M. Russwurm and J. W. Childers, *FT-IR open-path monitoring guidance document* (U.S. Environmental Protection Agency, Human Exposure and Atmospheric Sciences Division, National Exposure Research Laboratory, 1999).
21. Bruker, *D-fenceline™ and OPS*, https://brukeropenpath.com/atmosfir-d-fenceline/.
22. K. Numata, H. Riris, S. Li, S. Wu, S. R. Kawa, M. Krainak, and J. Abshire, "Ground demonstration of trace gas lidar based on optical parametric amplifier," J. Appl. Remote Sens. **6**(1), 063561 (2012).
23. J. Barrientos Barria, A. Dobroc, H. Coudert-Alteirac, M. Raybaut, N. Cézard, J.-B. Dherbecourt, T. Schmid, B. Faure, G. Souhaité, J. Pelon, J.-M. Melkonian, A. Godard, and M. Lefebvre, "Simultaneous remote monitoring of atmospheric methane and water vapor using an integrated path DIAL instrument based on a widely tunable optical parametric source," Appl. Phys. B: Lasers Opt. **117**(1), 509–518 (2014).
24. N. A. Macleod, R. Rose, and D. Weidmann, "Middle infrared active coherent laser spectrometer for standoff detection of chemicals," Opt. Lett. **38**(19), 3708–3711 (2013).
25. M. C. Phillips and B. E. Brumfield, "Standoff detection of turbulent chemical mixture plumes using a swept external cavity quantum cascade laser," Opt. Eng. **57**(1), 011003 (2017).
26. IEC 60825-1:2001, Edition 1.2, *Consolidated Edition; Safety of Laser Products—Part 1: Equipment classification, requirements and user's guide*.
27. O. Kara, L. Maidment, T. Gardiner, P. G. Schunemann, and D. T. Reid, "Dual-comb spectroscopy in the spectral fingerprint region using OPGaP optical parametric oscillators," Opt. Express **25**(26), 32713–32721 (2017).
28. L. Maidment, P. G. Schunemann, and D. T. Reid, "Molecular fingerprint-region spectroscopy from 5 to 12 µm using an orientation-patterned gallium phosphide optical parametric oscillator," Opt. Lett. **41**(18), 4261–4264 (2016).